Vol 17 No 5, May 2008
1674-1056/2008/17(05)/1743-09

Chinese Physics B

© 2008 Chin. Phys. Soc.
and IOP Publishing Ltd

Composite optical vortices in noncollinear Laguerre–Gaussian beams and their propagation in free space*

Cheng Ke(程 科), Liu Pu-Sheng(刘普生), and Lü Bai-Da(吕百达)†

Institute of Laser Physics and Chemistry, Sichuan University, Chengdu 610064, China

(Received 3 July 2007; revised manuscript received 9 September 2007)

Taking two Laguerre–Gaussian beams with topological charge $l = \pm 1$ as an example, this paper studies the composite optical vortices formed by two noncollinear Laguerre–Gaussian beams with different phases, amplitudes, waist widths, off-axis distances, and their propagation in free space. It is shown by detailed numerical illustrative examples that the number and location of composite vortices at the waist plane are variable by varying the relative phase β, amplitude ratio η, waist width ratio ξ, or off-axis distance ratio μ. The net topological charge $l_{\rm net}$ is not always equal to the sum $l_{\rm sum}$ of charges of the two component beams. The motion, creation and annihilation of composite vortices take place in the free-space propagation, and the net charge during the propagation remains unchanged and equals to the net charge at the waist plane.

Keywords: composite optical vortex, Laguerre–Gaussian beam, topological charge, creation and annihilation

PACC: 4225, 4225K

1. Introduction

Recently there has been substantial interest in studying optical beams carrying phase singularities due to their theoretical and applicative aspects.[1] Optical vortices nested in Gaussian beams, Bessel beams, second harmonic beams, partially coherent beams, and their propagation were studied.[1−9] Pyragaite and Stabinis[10] studied the free-space propagation of overlapping Gaussian background vortex beams and showed that the net topological charge of the combined beam remains unchanged. An extensive study of composite optical vortices by superimposing two noncollinear vortex Gaussian beams with equal topological charges $l_{1,2}$=+1, with opposite topological charges $l_{1,2} = \pm 1$ and by superimposing of a vortex and a Gaussian beam ($l_{1,2}$=+1, 0) at the waist plane was made by Maleev and Swartzlander,[11] who showed that, depending on the control parameter, such as the relative phase, amplitude, or distance between the component beams, the number of composite vortices and their net topological charge do not always correspond to the respective values for the component beams, but for the case of $l_{1,2} = \pm 1$ the net topological charge is always conserved. More recently, Galvez *et al* [12] performed a theoretical and experimental study of composite optical vortices formed by two collinear Laguerre–Gaussian beams and found that the number of vortices and their location depends on the charge of the vortices and the relative intensity of the component beams.

The purpose of the present paper is to deal with the composite optical vortices in noncollinear Laguerre–Gaussian beams. Taking two parallel and nonlinear Laguerre–Gaussian beams with $l_{1,2} = \pm 1$ and with different phases, amplitudes, waist widths and off-axis distances as an example, we study the composite optical vortices and their propagation in free-space and compare with the previous work.

2. Theoretical model

The field of a Laguerre–Gaussian beam with topological charge l_i in the cylindrical coordinate system reads as[1]

*Project supported by the National Natural Science Foundation of China (Grant No 10574097).

†Corresponding author. E-mail: baidalu0@tomcom

$$E(\rho_i,\theta_i,z) = E_{0i}\frac{w_{0i}}{w_i}\left(\frac{\sqrt{2}\rho_i}{w_i}\right)^{|l_i|}\exp\left(-\frac{\rho_i^2}{w_i^2}\right)L_{p_i}^{|l_i|}\left(\frac{2\rho_i^2}{w_i^2}\right) \times \exp\left\{\mathrm{i}\left[kz+\frac{k\rho_i^2}{2R_i(z)}+l_i\theta_i-(2p_i+|l_i|+1)\arctan\left(\frac{z}{z_{\mathrm{R}i}}\right)\right]\right\}, \quad (i=1,2), \tag{1}$$

where E_{0i} is an amplitude constant, w_{0i} is the waist width, $L_{p_i}^{|l_i|}(2\rho_i^2/\omega_i^2)$ denotes the Laguerre polynomial with azimuthal and radial indices l_i, p_i, $z_{\mathrm{R}i}=kw_{0i}^2/2$ is the Rayleigh length. $w_i=w_{0i}(1+z^2/z_{\mathrm{R}i}^2)^{1/2}$, and $R_i(z)=z(1+z_{\mathrm{R}i}^2/z^2)$ denote the width and radius of curvature at the z plane, respectively.

As shown in Fig.1, two Laguerre–Gaussian beams are located along the x axis and separated by distances a and $-b$ from the origin at the waist plane $z=0$ ($a>0$, $b>0$), respectively. The composite field is expressed as

$$E(\rho,\theta,z)=E(\rho_1,\theta_1,z)\exp(\mathrm{i}\beta)+E(\rho_2,\theta_2,z), \tag{2}$$

where β denotes the relative phase of the two beams at z=0, and the polar coordinates of the two component beams and composite beam satisfy the relation[11]

$$\rho_1\exp(\pm\mathrm{i}\theta_1)=\rho\exp(\pm\mathrm{i}\theta)-a, \tag{3a}$$

$$\rho_2\exp(\pm\mathrm{i}\theta_2)=\rho\exp(\pm\mathrm{i}\theta)+b. \tag{3b}$$

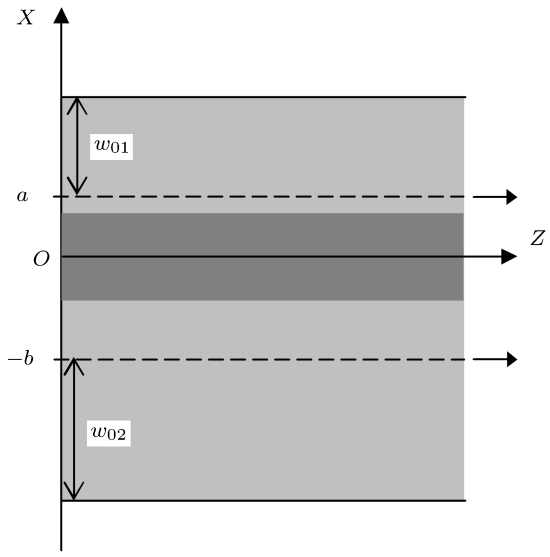


Fig.1. A schematic illustration of the superposition of two parallel and noncollinear beams.

In the following we restrict ourselves to the case of $p_1=p_2$=0, $l_1=-l_2$=+1. Thus, the sum of charges of the original beams is l_{sum}=0,[11] and Eq.(1) in the rectangular coordinate system can be written as

$$E(x,y,z)=E_1(x,y,z)\exp\{\mathrm{i}[\psi_1(x,y,z)+\beta]\} + E_2(x,y,z)\exp[\mathrm{i}\psi_2(x,y,z)], \tag{4}$$

where

$$E_1(x,y,z)=E_{01}\frac{\sqrt{2}(x-a+\mathrm{i}y)}{w_{01}(1+z^2/z_{\mathrm{R1}}^2)} \times \exp\left[-\frac{(x-a)^2+y^2}{w_{01}^2(1+z^2/z_{\mathrm{R1}}^2)}\right], \tag{5}$$

$$E_2(x,y,z)=E_{02}\frac{\sqrt{2}(x+b-\mathrm{i}y)}{w_{02}(1+w_{01}^4z^2/(w_{02}^4z_{\mathrm{R1}}^2))} \times \exp\left[-\frac{(x+b)^2+y^2}{w_{02}^2(1+w_{01}^4z^2/(w_{02}^4z_{\mathrm{R1}}^2))}\right], \tag{6}$$

$$\psi_1(x,y,z)=kz+\frac{k[(x-a)^2+y^2]}{w_{01}^2(z/z_{\mathrm{R1}}+z_{\mathrm{R1}}/z)} - 2\arctan(z/z_{\mathrm{R1}}), \tag{7}$$

$$\psi_2(x,y,z)=kz+\frac{k[(x+b)^2+y^2]}{w_{01}^2(z/z_{\mathrm{R1}}+w_{02}^4z_{\mathrm{R1}}/(zw_{01}^4))} - 2\arctan(zw_{01}^2/(w_{02}^2z_{\mathrm{R1}})). \tag{8}$$

Equations (4)–(8) are the free-space propagation expressions for composite optical vortices in noncollinear Laguerre–Gaussian beams with $p_1=p_2=0$ and $l_1=-l_2=+1$, where, as compared with Ref.[10], the propagation-induced phase terms Eqs.(7), (8) are included.

At the waist plane z=0 Eq.(4) reduces to

$$E(x,y,0)=E_{01}\frac{\sqrt{2}}{w_{01}}(x-a+\mathrm{i}y)\exp\left[-\frac{(x-a)^2+y^2}{w_{01}^2}+\mathrm{i}\beta\right]+E_{02}\frac{\sqrt{2}}{w_{02}}(x+b-\mathrm{i}y)\exp\left[-\frac{(x+b)^2+y^2}{w_{02}^2}\right]. \quad (9)$$

The location of composite vortices at z=0 is determined by Re[E(x, y, 0)]=0 and Im[E(x, y, 0)]=0, which yields

$$x=\frac{a\exp\left[-\frac{(x-a)^2+y^2}{w_{01}^2}+\mathrm{i}\beta\right]-\eta b\frac{w_{01}}{w_{02}}\exp\left[-\frac{(x+b)^2+y^2}{w_{02}^2}\right]}{\exp\left[-\frac{(x-a)^2+y^2}{w_{01}^2}+\mathrm{i}\beta\right]+\eta\frac{w_{01}}{w_{02}}\exp\left[-\frac{(x+b)^2+y^2}{w_{02}^2}\right]}, \quad (10a)$$

$$y\left\{\exp\left[-\frac{(x-a)^2+y^2}{w_{01}^2}+\mathrm{i}\beta\right]-\frac{w_{01}}{w_{02}}\exp\left[-\frac{(x+b)^2+y^2}{w_{02}^2}+\ln\eta\right]\right\}=0, \quad (10b)$$

where the amplitude ratio $\eta=E_{02}/E_{01}$.

Equations (10a) and (10b) indicate that for fixed p_1, p_2, l_1, l_2, the location and number of composite vortices and their net topological charge at the waist plane z=0 depend on the relative phase β, amplitude ratio η, waist width ratio $\xi=w_{01}/w_{02}$, and off-axis distance ratio $\mu=a/b$. As shown in Eq.(4), the location and number of composite vortices and their net topological charge at the z plane is additionally dependent on the propagation distance z.

For the special case of $w_{01}=w_{02}=w_0$, $a=b=s$ and $\sigma=s/w_0$, Eqs.(10a) and (10b) reduce to

$$x=s\tanh[2\sigma^2x/s+(1/2)\ln(E_{01}/E_{02})+\mathrm{i}\beta/2], \quad (11a)$$

$$y\sinh[2\sigma^2x/s+(1/2)\ln(E_{01}/E_{02})+\mathrm{i}\beta/2]=0. \quad (11b)$$

Equations (11a) and (11b) are consistent with Eqs.(18a) and (18b) in Ref.[11], respectively.

3. Composite optical vortices and their propagation in free space

By using Eqs.(4)–(10), we performed the numerical calculations to illustrate the dependence of the location and number of composite vortices and their net topological charge on β, η, w_{01}/w_{02}, a/b, and z.

3.1. Dependence on β and η

For simplicity we consider two cases of β=0 (in-phase), and β=π (out-of-phase). For β=0 the solutions of Eqs.(10a) and (10b) are given by

$$\begin{cases} y=0, \\ \eta=\dfrac{w_{02}}{w_{01}}\dfrac{a-x}{x+b}\exp\left[\dfrac{(x+b)^2}{w_{02}^2}-\dfrac{(x-a)^2}{w_{01}^2}\right], \end{cases} \quad (12a)$$

$$\begin{cases} x=(a-b)/2, y\neq 0, \\ \eta=\dfrac{w_{02}}{w_{01}}\exp\left[\left(\dfrac{1}{w_{02}^2}-\dfrac{1}{w_{01}^2}\right)\left(\dfrac{(a+b)^2}{2}+y^2\right)\right]. \end{cases} \quad (12b)$$

Figures 2(a) and 2(b) give the variation of η versus x or y at the waist plane z=0. The calculation parameters are a=0.5mm, b=1mm, $w_{01}=\sqrt{2}$mm, w_{02}=2mm. Figure 2(a) indicates that η varies with x in a monodromic way, there is only one vortex corresponding to Eq.(12a), whereas, as shown in Fig.2(b), there exists a critical value of η=η_c=1.23 in Eq.(12b). For $0<\eta<\eta_c$ there are two vortices, and for $\eta\geq\eta_c$ the vortex vanishes. As a result, for $0<\eta<\eta_c$ there are three vortices, and for $\eta\geq\eta_c$, there is one vortex.

For $\beta=\pi$ the solutions of Eqs.(10a) and (10b) are

$$\begin{cases} y=0, \\ \eta=\dfrac{w_{02}}{w_{01}}\dfrac{x-a}{x+b}\exp\left[\dfrac{(x+b)^2}{w_{02}^2}-\dfrac{(x-a)^2}{w_{01}^2}\right]. \end{cases} \quad (13)$$

The variation of η versus x is plotted in Fig.2(c), from which we see that there exists a critical value of η=η_c=2.34, we have three vortices and one vortex for $0<\eta<\eta_c$ and $\eta\geq\eta_c$, respectively.

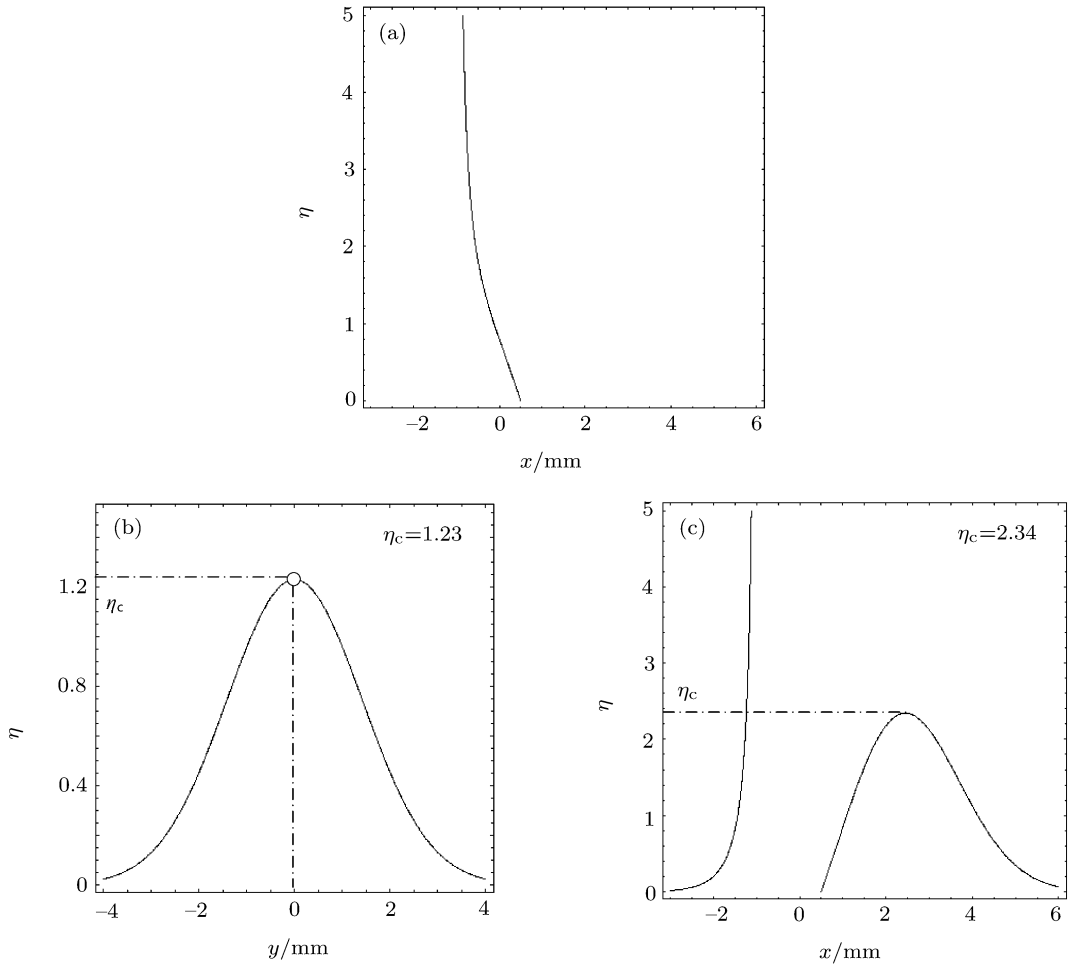


Fig.2. Amplitude ratio η versus coordinate x or y at z=0.

The phase maps at the waist plane z=0 are plotted in Figs.3 (β=0) and 4 (β=π) for different values of η, where the solid lines are zeros of the real part of $E(x, y, 0)$ and the dashed lines are zeros of the imaginary part of $E(x, y, 0)$. The zero contours of the real and imaginary parts intersect at composite vortex points. The calculation parameters are the same as those in Figs.2(a)–2(c). The topological charge of composite vortices is determined by the vorticity of phase contours around singularities.[13] Black and open circles mark the cores of positively and negatively single-charged vortices, respectively. As can be seen, in Fig.3 (η=1) there are three composite vortices A, B and C, whose charges are +1, –1 and –1, respectively. In Fig.4(a) (η=1) there are three vortices A, B and C with charges –1, +1 and –1, respectively, and in Fig.4(b) there is one vortex A with charge –1. It is noted that at the critical point B denoted by a cross '×' the real part Re[$E(x, y, 0)$] becomes a point which can be seen from Fig.2(c), but B is not a vortex, because, as can be seen from the phase maps, the phase is not rotating around the point B. Therefore,

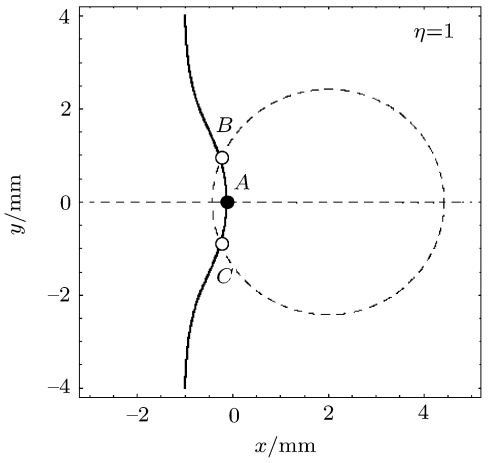


Fig.3. Phase maps at z=0 for different values of the amplitude ratio η, β=0, η=1. '—' Re[$E(x, y, 0)$]=0, '- - - -' Im[$E(x, y, 0)$]=0.

depending on the relative phase β=0 or π, and on the amplitude ratio $0 < \eta < \eta_c$ or $\eta \geq \eta_c$, the number of composite vortices at z=0 may be one or three. Figures 3, 4(a) and 4(b) indicate l_{net}=–1 that is unequal to l_{sum}=0.

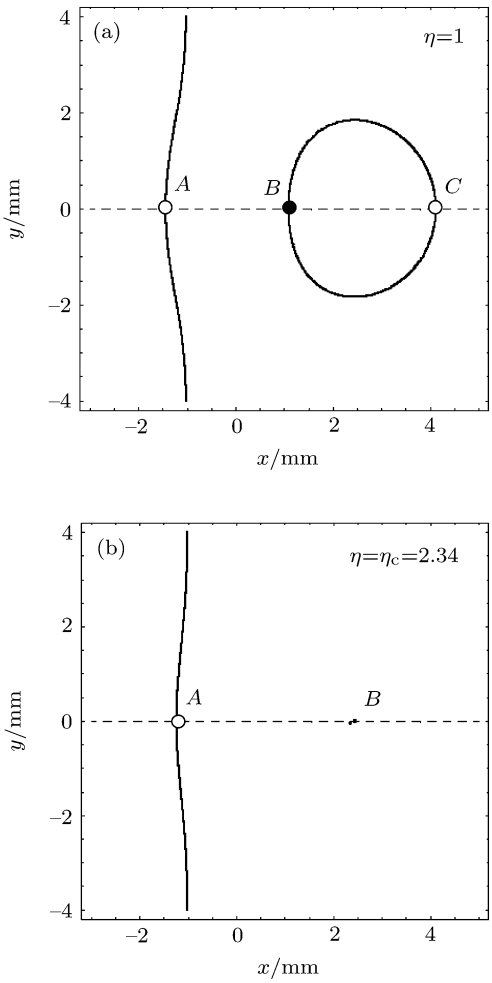


Fig.4. Phase maps at z=0 for different values of the amplitude ratio η, β=π. (a) η=1, (b) η=2.34. '—' Re[$E(x, y, 0)$]=0, '- - - -' Im[$E(x, y, 0)$]=0.

3.2. Dependence on β and ξ

The variation of ξ as a function of the transversal coordinate x or y is depicted in Figs.5(a) and 5(b) for β=0 and in Fig.5(c) for β=π at the waist plane z=0. The corresponding phase maps at the waist plane z=0 are given in Fig.6 for β=0 and Figs.7(a)–7(b) for β=π, where the calculation parameters are a=0.5mm, b=1mm, η=10, w_{02}=2mm. It is seen that in Fig.6 for β=0, $\xi = 1.5 > \xi_c$=1.003 the number of composite vortices is three with l=–1, –1, +1. Thus, l_{net}=–1≠ l_{sum}=0. For β=π the critical value of the waist width ratio is ξ_c=0.875. Depending on ξ, we find that there is one composite vortex A with l=–1 in Fig.7(a) ξ=ξ_c=0.875, and three composite vortices A, B, C with l=–1, +1 and +1 in Fig.7(b) $\xi = 1.5 > \xi_c$. Again, the critical point B in Fig.7(a) is not a vortex.

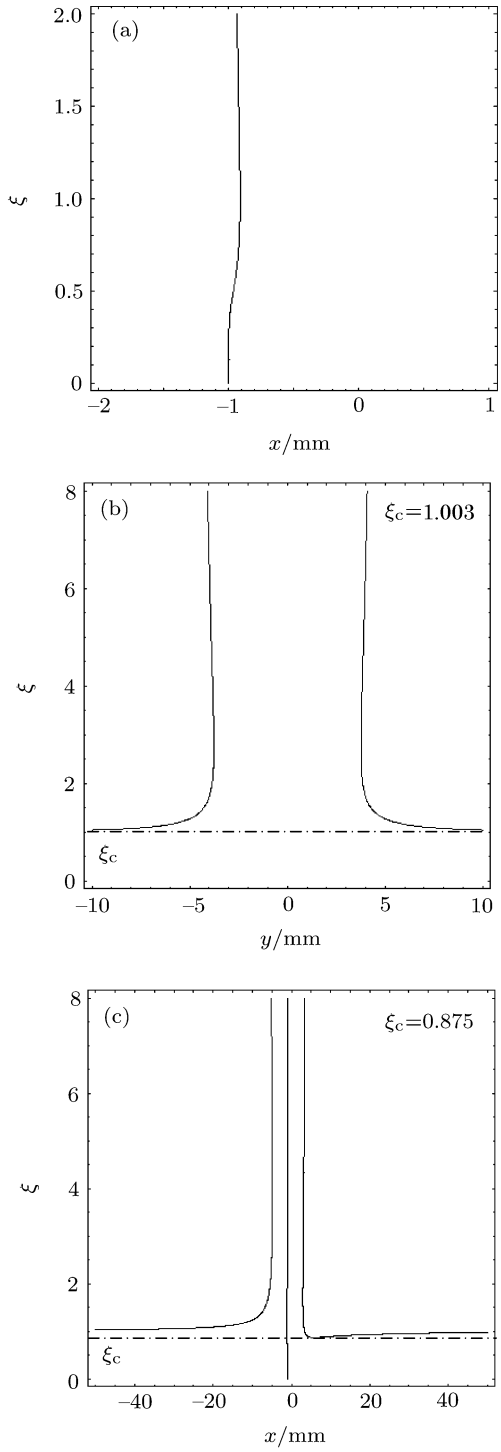


Fig.5. Waist width ratio ξ versus coordinate x or y at z=0.

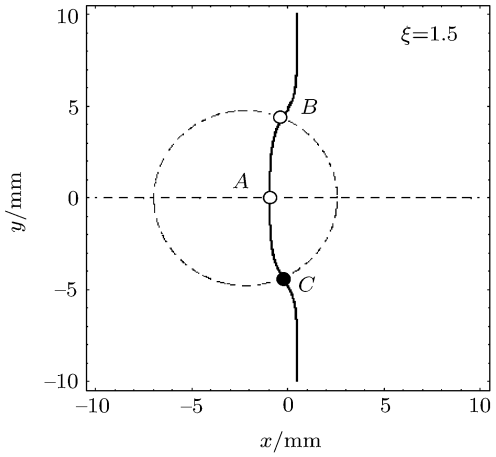


Fig.6. Phase maps at z=0 for different values of the waist width ratio ξ, β=0. ξ=1.5. '—' Re[$E(x, y, 0)$]=0, '- - - -' Im[$E(x, y, 0)$]=0.

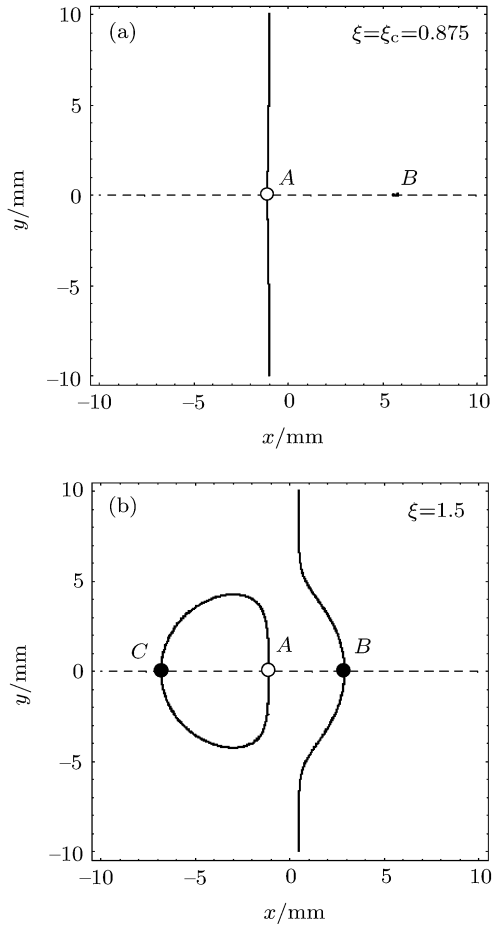


Fig.7. Phase maps at z=0 for different values of the waist width ratio ξ, β=π. (a)ξ=0.875, (b)ξ=1.5. '—' Re[$E(x, y, 0)$]=0, '- - - -' Im[$E(x, y, 0)$]=0.

3.3. Dependence on β and μ

Figures 8(a) and 8(b) give the variation of μ versus x or y for β=0 and π at the waist plane z=0, respectively. The calculation parameters are b=1mm, η=10, w_{01} = $\sqrt{2}$mm, w_{02}=2mm. In such a case Eq.(12b) has no real solution. It is seen that there are two critical parameters of the off-axis distance ratio μ_{1c} and μ_{2c}. For β=0, we have μ_{1c}=–5.58 and μ_{2c}=3.59. In the region $\mu_{1c} \le \mu \le \mu_{2c}$ there is one composite vortex. If $\mu < \mu_{1c}$ or $\mu > \mu_{2c}$, there are three vortices. For $\beta = \pi$ we have μ_{1c}=–3.29 and μ_{2c}=1.28 and obtain similar results. The corresponding phase maps at z=0 are depicted in Figs.9 (β=0) and 10 ($\beta = \pi$), from which we see that the number of composite vortices may be one or three, depending on β and μ. For the case of $\mu_{1c} \le \mu \le \mu_{2c}$ in Fig.9(a) and Fig.10(a) there is one composite vortex A with l=–1. For the case of $\mu < \mu_{1c}$ or $\mu > \mu_{2c}$ in Fig.9(b) and Fig.10(b), there are three vortices with $l_{\rm net}$=–1.

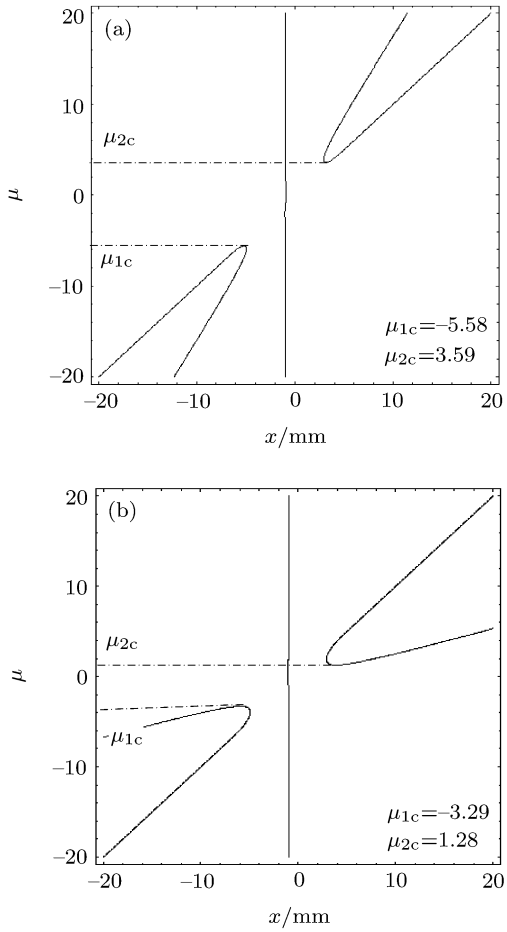


Fig.8. Off-axis distance ratio μ versus coordinate x or y at z=0.

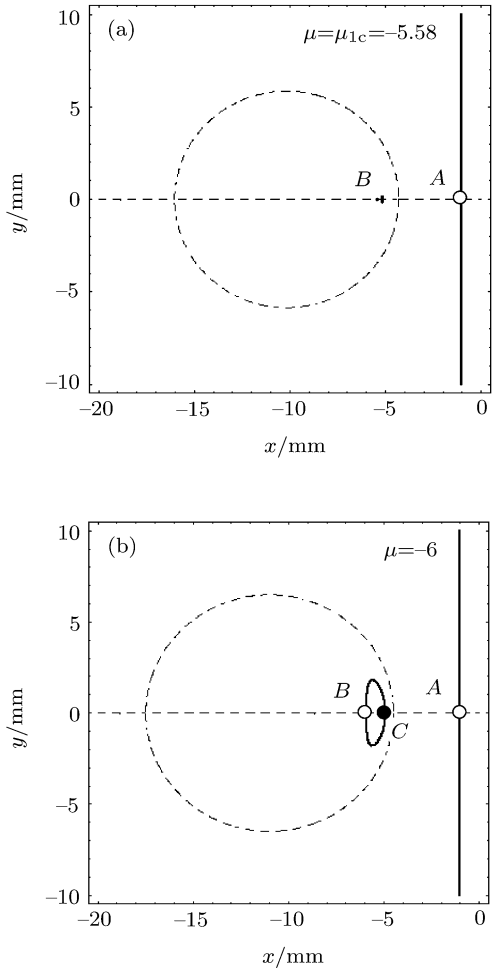


Fig.9. Phase maps at z=0 for different values of the off-axis distance ratio μ, β=0. (a)μ=–5.58, (b) μ=–6. '—' Re[$E(x, y, 0)$]=0, '- - - -' Im[$E(x, y, 0)$]=0.

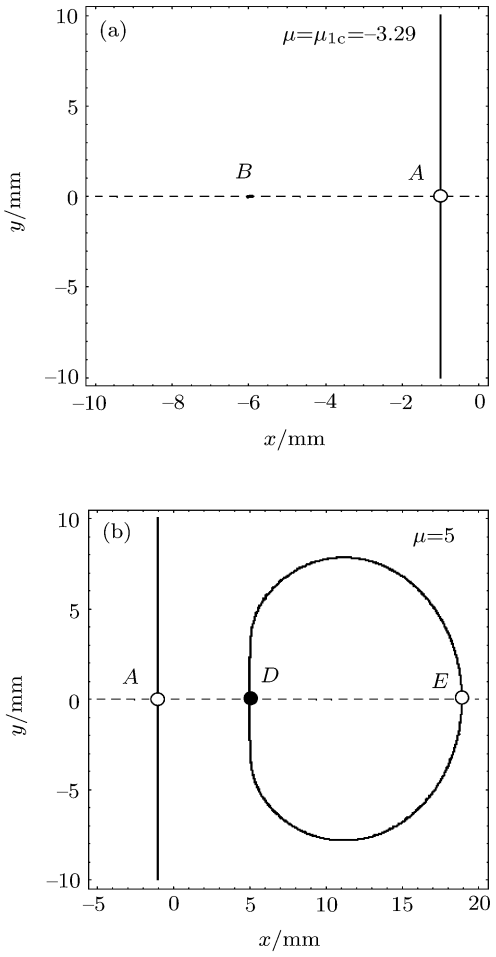


Fig.10. Phase maps at z=0 for different values of the off-axis distance ratio μ, $\beta=\pi$. (a) μ=–3.29, (b) μ=5. '—' Re[$E(x, y, 0)$]=0, '- - - -' Im[$E(x, y, 0)$]=0.

3.4. Free space propagation of composite optical vortices

The variation of composite optical vortices versus propagation distance z in free space is given in Figs.11(a)–11(c) for β=0 and in Figs.12(a)–12(c) for $\beta=\pi$, respectively, where the calculation parameters are the same as those in Fig.3 and Fig.4(a), respectively. Figures 3 and 11(a)–(c) show that the creation and annihilation of composite vortices take place during propagation. For example, composite vortices A, B, C moves from positions (x=–0.15mm, y=0), (x = −0.25mm, y = 0.8mm), (x = −0.25mm, y=–0.8mm) at the waist plane z=0 in Fig.3 to A (x=–0.5mm, y=0.7mm), B (x=2.1mm, y=3.5mm), C (x=5.6mm, y=–3.6mm) at the plane z/z_{R1}=0.8 in Fig.11(a) whose charge are –1, +1 and –1, respectively. At z/z_{R1}=0.9 in Fig.11(b) A, B, C move to the positions (x=–0.55mm, y=0.8mm), (x=1.8mm, y=3.7mm) and (x=4.9mm, y=–4.9mm), respectively, and their charge remains unchanged. In addition, two composite vortices D with l=+1 and E with l=–1 appear at the positions (x=8.5mm, y=3.2mm) and (x=9.7mm, y=–1.7mm), respectively. With a further increase of z/z_{R1}=4 in Fig.11(c), vortices D and E annihilate and the other three vortices A (x=–0.6mm, y=0), B (x=1mm, y=6.1mm) and C (x=–8.2mm, y=3.5mm) remain.

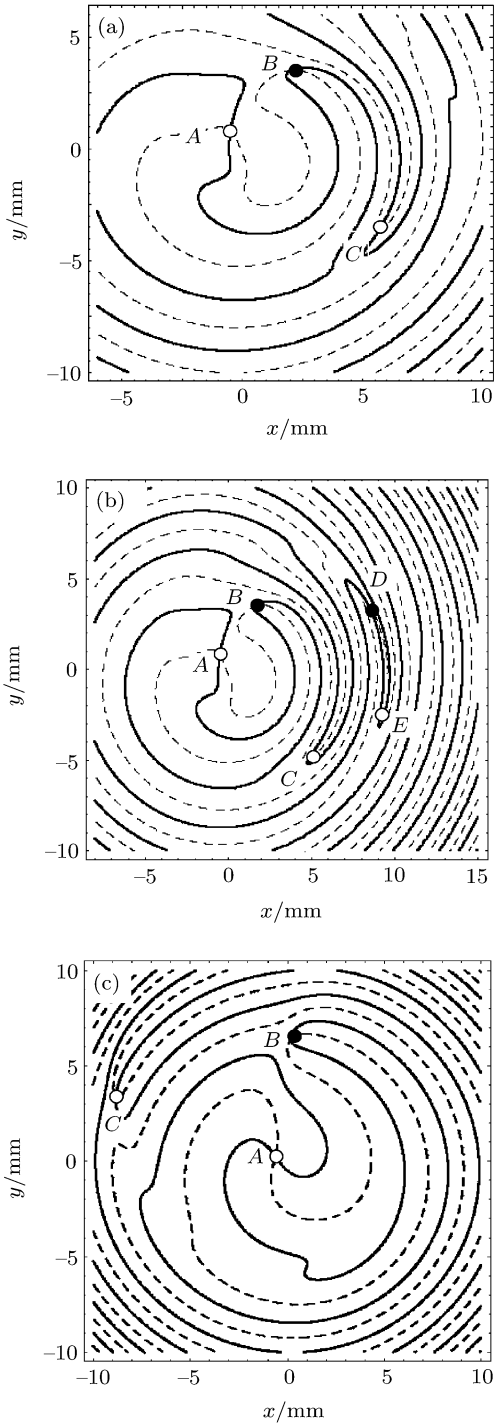


Fig.11. Phase maps for different values of the propagation distance. (a) z/z_{R1}=0.8, (b) z/z_{R1}=0.9, (c) z/z_{R1}=4, β=0. '—' Re[$E(x, y, z)$]=0, '- - - -' Im[$E(x, y, z)$]=0.

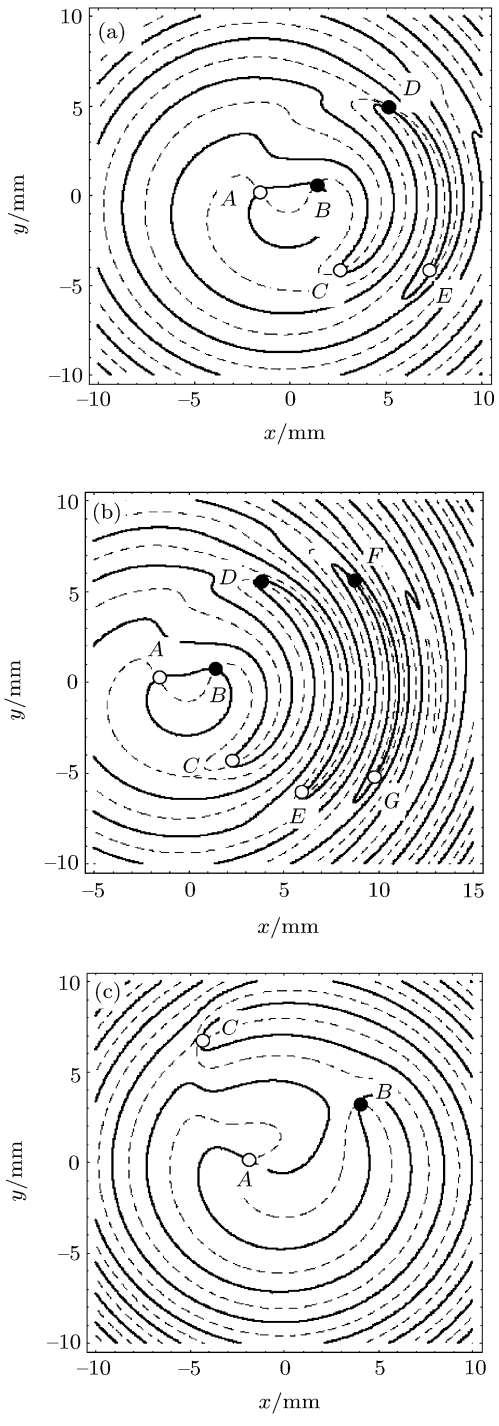


Fig.12. Phase maps for different values of the propagation distance. (a) z/z_{R1}=0.9, (b) z/z_{R1}=1, (c) z/z_{R1}=4, β=π. '—' Re[$E(x, y, z)$]=0, '- - - -' Im[$E(x, y, z)$]=0.

Similar results are seen in Figs.4(a) and 12(a)–(c) for β=π. The positions of vortices A, B and C at the waist plane z=0 in Fig.4(a) are (x=–1.5mm, y=0), (x=1.1mm, y=0), (x=4.2mm, y=0), respectively. As can be seen from Fig.12(a), there are five composite vortices A (x=–1.5mm, y=0.4mm), B (x=1.6mm, y=0.6mm), C (x=2.6mm, y=–4.1mm), D (x=4.8mm, y=5.0mm) and E (x=7.5mm, y=–4mm), with l=–1, +1, –1, +1 and –1, respectively at z/z_{R1}=0.9. Vortices A, B, C, D, E move to the positions (x=–1.8mm,

y=0.2mm), (x=1.3mm, y=0.6mm), (x=2.2mm, y=–4.5mm), (x=3.7mm, y=5.5mm) and (x=5.8mm, y=–6.2mm), respectively, and additional two vortices F (x=8.5mm, y=5.7mm), G (x=9.9mm, y=–5.1mm) with l=+1, –1 appear at $z/z_{\rm R1}$=1 in Fig 12(b). Increasing $z/z_{\rm R1}$ to 4, we find that vortices D, E, F, G disappear and there are three vortices A (x=–2mm, y=0.2mm), B (x=3.5mm, y=3.1mm) and C (x=–4.5mm, y=5.7mm). Therefore, it follows from Figs.11 and 12 that in the free space propagation the number and location of composite vortices vary, i.e., composite vortices move, create and annihilate, but their net topological charge $l_{\rm net}$=–1 is conserved and equals to the net charge at the waist plane z=0.

4. Conclusions

This paper makes a detailed study of composite optical vortices formed by two parallel and noncollinear Laguerre–Gaussian beams and their propagation in free space in the more general case, where the amplitude, phase, waist width and off-axis distance of the two component beams are not equal. Analytical and numerical results have shown that the number and location of composite vortices at the waist plane z=0 depend not only on the relative phase and distance,[11] but also on the amplitude ratio, waist width ratio and off-axis distance ratio. The net topological charge $l_{\rm net}$ of composite vortices is not always equal to the sum $l_{\rm sum}$ of charges of the two component beams. In the free-space propagation the motion, creation and annihilation of composite vortices appear. The net charge during the propagation is conserved and equals to that at the waist plane z=0. For the case of the equal waist width ratio ξ=1 and equal off-axis distance ratio μ=1, Eqs.(10a) and (10b) reduce to Eqs.(18a) and (18b) in Ref.[11], and the same results like Figs.5 and 6 in Ref.[11] can be obtained. It means that only under such conditions the net topological charge at the waist plane z=0 is conserved. For clarifying the main results, two Laguerre–Gaussian beams with $p_{1,2}$=0, $l_{1,2}=\pm1$ have been taken as an example. It is shown that for the other cases, i.e., two Laguerre–Gaussian beams with $p_{1,2}$=0, $l_{1,2}$=+1 or $l_{1,2}$=–1, 0, the approach in this paper is applicable and similar conclusions can be drawn.

References

[1] Soskin M S and Vasnetsov M V 2001 *Progress in Optics* **42** 219
[2] Indebetouw G 1993 *J. Mod. Opt.* **40** A73
[3] Orlov S and Stabinis A 2003 *Opt. Commun.* **226** 97
[4] Orlov S and Stabinis A 2004 *J. Opt.* A: *Pure Appl. Opt.* **6** S259
[5] Orlov S, Regelskis K, Smilgevicius V and Stabinis A 2003 *Opt. Commun.* **215** 1
[6] Orlov S, Regelskis K, Smilgevicius V and Stabinis A 2004 *J. Opt.* A: *Pure Appl. Opt.* **6** S255
[7] Gabriel M T and Torner L 2000 *J. Opt. Soc. Am.* B **17** 1197
[8] Liu P S and Lü B D 2007 *Chin. Phys.* **16** 411
[9] Liu P S and Lü B D 2007 *Acta Phys. Sin.* **56** 2623 (in Chinese)
[10] Pyragaite V and Stabinis A 2002 *Opt. Commun.* **213** 187
[11] Maleev I D and Swartzlander G A 2003 *J. Opt. Soc. Am.* B **20** 1169
[12] Galvez E J, Smiley N and Fernandes N 2006 *Proc. SPIE* **6131** 613105
[13] Freund I and Shvartsman N 1994 *Phys. Rev.* A **50** 5164